



# Quantifying the constraint of biospheric process parameters by CO<sub>2</sub> concentration and flux measurement networks through a carbon cycle data assimilation system

E. N. Koffi<sup>1,\*</sup>, P. J. Rayner<sup>2</sup>, M. Scholze<sup>3</sup>, F. Chevallier<sup>1</sup>, and T. Kaminski<sup>4</sup>

<sup>1</sup>Laboratoire des Sciences du Climat et de l'Environnement (LSCE), UMR8212, Ormes des merisiers, 91191 Gif-sur-Yvette, France

<sup>2</sup>School of Earth Sciences, University of Melbourne, Melbourne, Australia

<sup>3</sup>School of Earth Sciences, University of Bristol, Queen's Road, Bristol BS8 1RJ, UK

<sup>4</sup>FastOpt, Lerchenstraße 28a, 22767 Hamburg, Germany

\* now at: the European Commission Joint Research Centre, Institute for Environment and Sustainability, 21027 Ispra (Va), Italy

Correspondence to: E. N. Koffi (ernest.koffi@jrc.ec.europa.eu)

Received: 28 April 2012 – Published in Atmos. Chem. Phys. Discuss.: 14 September 2012

Revised: 2 September 2013 – Accepted: 30 September 2013 – Published: 1 November 2013

**Abstract.** The sensitivity of the process parameters of the Biosphere Energy Transfer HYdrology (BETHY) model to choices of atmospheric concentration network, high frequency terrestrial fluxes, and the choice of flux measurement network is investigated by using a carbon cycle data assimilation system. We use BETHY-generated fluxes as a proxy of flux measurements. Results show that monthly mean or low-frequency observations of CO<sub>2</sub> concentration provide strong constraints on parameters relevant for net flux (NEP) but only weak constraints for parameters controlling gross fluxes. The use of high-frequency CO<sub>2</sub> concentration observations, which has led to great refinement of spatial scales in inversions of net flux, adds little to the observing system in the Carbon Cycle Data Assimilation System (CCDAS) case. This unexpected result is explained by the fact that the stations of the CO<sub>2</sub> concentration network we use are not well placed to measure such high frequency signals. Indeed, CO<sub>2</sub> concentration sensitivities relevant for such high frequency fluxes are found to be largely confined in the vicinity of the corresponding fluxes, and are therefore not well observed by background monitoring stations. In contrast, our results clearly show the potential of flux measurements to better constrain the model parameters relevant for gross primary productivity (GPP) and net primary productivity (NPP). Given

uncertainties in the spatial description of ecosystem functions, we recommend a combined observing strategy.

## 1 Introduction

Uncertainties in the distribution of the carbon flux in the atmosphere limit both the skill of predictive models and the application of carbon accounting using measurements. Given the importance of this problem, various sources of measurements (including dedicated satellite missions) are available and quite sophisticated systems have been built to use them. There are two main approaches: the simplest are direct inversion systems in which atmospheric transport models and Bayesian estimation methods are used to infer surface fluxes from atmospheric CO<sub>2</sub> concentrations. These have been broadly used but their estimates vary widely due to differences in setup, observational data, prior estimates of the fluxes and transport models (e.g., Gurney et al., 2002, 2004; Law et al., 2003; Baker et al., 2006; Rayner et al., 2008; Chevallier et al., 2010). A second approach uses a range of observations to constrain the possible trajectories of dynamical models of the carbon cycle. The process parameters of the dynamical model are first constrained and then the optimized model is used to predict the various quantities of interest. The

uncertainties in the parameters of the dynamical model are projected forward into the output of the model constrained by the observations. Because of the use of an explicit dynamical carbon model, this approach is often termed carbon-cycle data assimilation (analogous to data assimilation in numerical weather prediction). The trade-offs between these two approaches are discussed in Kaminski et al. (2002).

The Carbon Cycle Data Assimilation System (CCDAS) used in the present work has two primary components:

- i. A deterministic dynamical model that calculates the evolution of both the biosphere and soil fluxes given an initial condition, forcing and a set of process parameters of the model.
- ii. An assimilation system that consists of an algorithm to adjust a subset of the state variables, initial conditions and/or process parameters to reduce the mismatch with observations. Usually any prior information on the variables which are adjusted are also taken into account (see Kaminski et al., 2002, 2003; Rayner et al., 2005, and references therein for the underlying methodology).

The CCDAS can ingest many types of observations, e.g., atmospheric CO<sub>2</sub> (Rayner et al., 2005; Scholze et al., 2007; Koffi et al., 2012), fAPAR (fraction of absorbed photosynthetically active radiation) and atmospheric CO<sub>2</sub> together (Kaminski et al., 2012a), satellite-derived fAPAR at site level alone (Knorr et al., 2010) and its combination with eddy-correlation fluxes (Kato et al., 2013). It has proven difficult to assimilate multiple observations simultaneously, suggesting inconsistencies between the information in the data streams and the model. To some extent this inconsistency is probably due to limitations in state-of-the-art models (Rayner, 2010). Models are, however, improving all the time, with recent success in transferring information from one site to another (a precondition for general success) (Medvigy et al., 2009). Thus, it is worth revisiting the constraint available from observations beyond the monthly mean concentrations hitherto used in global studies (Rayner et al., 2005; Koffi et al., 2012).

One motivation for such an exploration is recent advances in the use of high-frequency observations of CO<sub>2</sub> concentration in direct inversions. Law et al. (2003), Peylin et al. (2005), Peters et al. (2007, 2010), Zupanski et al. (2007), Lauvaux et al. (2009a, b), and Carouge et al. (2010a, b) have shown that there is considerable information on the distribution of CO<sub>2</sub> sources and sinks retrievable from the time series of concentrations. There are reasons for optimism and pessimism when applying continuous observations to the constraint of model parameters (the CCDAS approach). On the positive side is the obvious analogy between the direct inversion and the CCDAS methods, which both rely on information about fluxes. Furthermore, the time variations in fluxes themselves (such as the response to changes in photosynthetically active radiation forced by changing cloudiness) may

allow the roles of particular parameters to be probed, even though model errors are strongly correlated in time (Chevallier et al., 2012). The major dampener on our optimism is the inherent difference in scales implicit in the two approaches. CCDAS systems such as Rayner et al. (2005) constrain a small number of parameters (57 in that case). These modulate, via the model dynamics, structures in flux and hence concentration. For the majority of parameters their spatial impact extends across the coverage of a particular plant functional type (PFT). Other parameters have a global impact since they apply to plants or soils everywhere. The main impact of continuous observations in direct flux inversions has been a refinement of scale, an advantage that may not apply in a CCDAS system. However, as noted by Rayner et al. (2005) and Koffi et al. (2012), there are still many unconstrained parameters in CCDAS systems when using monthly atmospheric CO<sub>2</sub> concentration, so it is worth asking the question whether higher resolution of such data may help to constrain them better.

There is another major dataset available on the terrestrial carbon cycle in the form of continuous measurements of fluxes at very small scales (e.g., Foken and Wichura, 1996; Aubinet et al., 2000; Baldocchi, 2003; Rebmann et al., 2005; Reichstein et al., 2005; Papale et al., 2006; Lasslop et al., 2010; Kuppel et al., 2012; and references therein). Recently, Williams et al. (2009) reviewed the use of the international flux measurement network FLUXNET data (Baldocchi, 2003) for improving land surface models. These have afforded much information on processes affecting the terrestrial carbon-cycle (e.g., Ciais et al., 2005; Piao et al., 2008). They have been used in various assimilation efforts (e.g., Wang et al., 2001; Knorr and Kattge, 2005; Medvigy et al., 2009). They have also been tested in a simplified assimilation system (Kaminski et al., 2002) where they showed a large reduction in parameter uncertainty. Knorr et al. (2010) used satellite-derived fAPAR at site level alone and Kato et al. (2013) combined it with eddy-correlation flux measurements of latent heat in a full CCDAS. Kaminski et al. (2012b) also used the full CCDAS to assess and analyze the constraint of observational networks composed of continuous flux measurements, and daily and monthly atmospheric concentration measurements. In particular they demonstrated, within the model framework, the power of a small flux network to observe a region, provided that the network is complete, i.e., that it covers every plant functional type (PFT). They also demonstrated the complementarity of atmospheric networks to flux networks, in particular incomplete ones. That study did not, however, exploit the full power of the biosphere model since it did not consider at least the day-to-day variations of flux in response to radiation and temperature. These variations are likely to reveal different sensitivities of fluxes and concentrations that can provide additional constraints on carbon model parameters. Thus, our tasks here are to use daily forcing data to assess, within a theoretical framework, the power of continuous concentration and flux observations

to constrain model parameters; and, if the constraint is useful, to understand the sources of the information in the measurements and make recommendations for their use. For the flux measurements, we use as a proxy the generated fluxes of the Biosphere Energy Transfer HYdrology (BETHY) model.

To achieve the above mentioned objectives, we use the CCDAS (Rayner et al., 2005) built around the biosphere model BETHY (Biosphere Energy Transfer HYdrology) and some functionalities of the general Bayesian optimization PYthon VARIational (PYVAR; Chevallier et al., 2005) system. The outline of the paper is as follows: we describe in Sect. 2 the main pieces that compose both CCDAS and the PYVAR assimilation system. The formalism used to compute the uncertainty in parameters of the biosphere model is defined in Sect. 3. The data are described in Sect. 4. The different model/data configurations used to achieve the objectives of the paper are detailed in Sect. 5. The constraint of the parameters available from (i) high frequency observations of CO<sub>2</sub> concentrations, (ii) BETHY daily flux integrals, and (iii) BETHY hourly generated fluxes as a proxy of flux measurements are given in Sect. 6. In Sect. 7, results are discussed. Finally, conclusions are presented in Sect. 8.

## 2 Assimilation systems

In this section, we describe both the CCDAS and PYVAR system and how their elements are combined to fulfil the objectives of the paper.

### 2.1 Overall methodology

Our task is to quantify the information content of various sources of measurements that can be ingested by an assimilation system. We quantify the information by the reduction in the uncertainty of model parameters, operationally defined using the ratio of posterior and prior standard deviations. Under the linear Gaussian assumption, the posterior uncertainty is dependent only on the prior uncertainty, the assumed uncertainty for the measurements, and the sensitivity of the simulated observations to changes in the parameter (usually called the Jacobian). Thus, the main technical task described below is the calculation of these Jacobians for various classes of observations. A flow chart of the methodology is given in Fig. 1 and described in detail in following sections.

### 2.2 CCDAS

CCDAS combines the biosphere model BETHY (Knorr, 2000) and an atmospheric transport model. We use the version of Koffi et al. (2012), which includes the atmospheric model TM3 (Heimann and Körner, 2003). The process parameters of BETHY we use are summarized in Table 1. Note that Kaminski et al. (2012b) used the same process parameters, but different values, taken from an optimization by

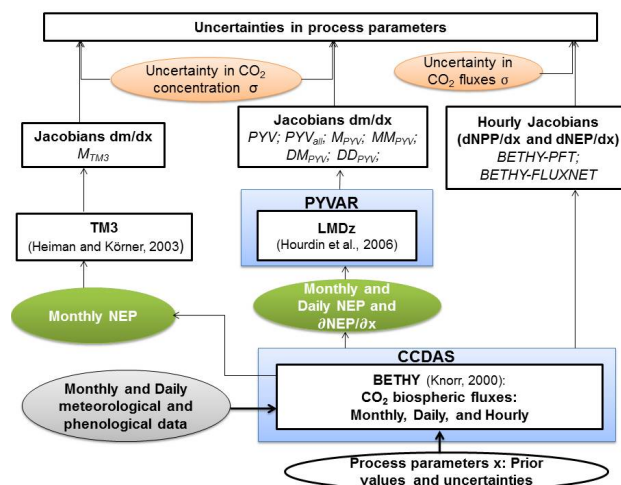


**Fig. 1.** Methodology used to calculate the uncertainties in the process parameters of BETHY when using different temporal resolutions of meteorological and phenological data to compute the biospheric fluxes, as well as two different types of data (i.e., CO<sub>2</sub> concentration and flux) to constrain these parameters. Flow chart shows the different settings (i.e.,  $M_{TM3}$ , PYV,  $PYV_{all}$ ,  $M_{PYV}$ ,  $MM_{PYV}$ ,  $DM_{PYV}$ ,  $DD_{PYV}$ , BETHY-PFT, BETHY-FLUXNET) used to investigate the sensitivities of the process parameters to (i) the temporal resolutions of both meteorological and phenological data and the modeled BETHY fluxes (i.e., NPP and NEP), and (ii) the type of measurements, as described in Sect. 5.  $m$  stands for the simulated CO<sub>2</sub> concentration, as used in the Eq. (1). The uncertainties in the observations are characterized by the standard deviation  $\sigma$ . The acronyms CCDAS and PYVAR are described in Sect. 2. Note that for the sake of clarity, the transport model TM3 is not put in the block of CCDAS, as described in Sect. 2.2.

Scholze et al. (2007) against a different observational network and with a different transport model.

BETHY is a process-based model of the terrestrial biosphere that simulates carbon assimilation and plant and soil respiration, embedded within a full energy and water balance (Knorr, 2000). BETHY uses 13 plant functional types (PFTs; see Fig. 2). The base temporal resolution of BETHY simulation is 1 h, but one day is used for variables related to soil respiration. A grid cell can contain up to three different PFTs, with the amount specified by their fractional coverage. A complete description of BETHY for the assimilation of CO<sub>2</sub> concentrations is given in Rayner et al. (2005) and the version used in this study is detailed in Koffi et al. (2012). Therefore, we briefly define the BETHY fluxes together with their relevant parameters, which we use later. BETHY computes the gross primary productivity (GPP) using the parameterizations of Farquhar et al. (1980) and Collatz et al. (1992) for C3 and C4 plants, respectively. The net primary productivity (NPP) is computed as a gross uptake of CO<sub>2</sub> by the leaves (GPP) minus total autotrophic respiration, which includes plant maintenance respiration and growth respiration. Then, the net CO<sub>2</sub> flux between the atmosphere and the net

**Table 1.** Controlling parameters of the biosphere model BETHY and their prior values: Units are  $V_{\max}$ ,  $\mu\text{mol}(\text{CO}_2) \text{ m}^{-2} \text{ s}^{-1}$ ;  $a_{J,T}$  activation parameter ( $\text{C}^{-1}$ );  $a_{\Gamma,T}$   $\mu\text{mol}(\text{CO}_2) \text{ mol}(\text{air})^{-1}(\text{C})^{-1}$ ; activation energies  $E$ ,  $\text{J mol}^{-1}$ ; and  $\tau_f$ , years; all other parameters are unitless and correspond to values at 25 °C.  $K_C$  is multiplied by  $10^6$ . These parameters have been optimized by Koffi et al. (2012) and widely described in Rayner et al. (2005). Gaussian PDFs are used for the 14 parameters marked with the asterisk symbol, i.e.,  $a_{\Gamma,T}$ ,  $a_{J,V}$  (PFT dependent, thus 13 parameters); for all others a log-normal PDF is assumed. The definitions of the acronyms of the PFTs are given in the caption of Fig. 2. The parameters related to gross primary productivity (GPP) are  $V_{\max}$ ,  $a_{J,V}$ ,  $E_{V_{\max}}$ ,  $E_{K_o}$ ,  $E_{K_c}$ ,  $E_k$ ,  $\alpha_q$ ,  $\alpha_i$ ,  $K_C$ ,  $K_o$ , and  $a_{\gamma,T}$ ; those related to the net primary productivity NPP are  $f_{R_{\text{leaf}}}$ ,  $f_{R_{\text{growth}}}$ , and  $E_{R_d}$ . Note that  $f_{R_{\text{leaf}}}$  (leaf respiration) and  $f_{R_{\text{growth}}}$  (growth respiration) are also linked to the autotrophic respiration. The parameters relevant for the net flux NEP are  $\beta$ ,  $Q_{10f}$ ,  $Q_{10s}$ ,  $\tau_f$ ,  $\kappa$ , and  $f_s$ , among which  $Q_{10f}$ ,  $Q_{10s}$ ,  $\tau_f$ ,  $\kappa$ , and  $f_s$  parameters are also linked to the heterotrophic respiration.

Parameters	Prior values	Prior uncertainty	Parameters	Prior values	Prior uncertainty
$V_{\max}$ (TrEv)	60.	12.	$Q_{10f}$	1.5	1.5
$V_{\max}$ (TrDec)	90.	18.	$Q_{10s}$	1.5	1.5
$V_{\max}$ (TmpEv)	41.	8.2	$\tau_f$	1.5	3.0
$V_{\max}$ (TmpDec)	35.	7.	$\kappa$	1.	10.0
$V_{\max}$ (EvCn)	29.	5.8	$f_s$	0.2	2.0
$V_{\max}$ (DecCn)	53.	10.6	$E_{R_d}$	45 000.	2250.0
$V_{\max}$ (EvShr)	52.	10.4	$E_{V_{\max}}$	58 520.	2926.0
$V_{\max}$ (DecShr)	160.	32.	$E_{K_o}$	35 948.	1797.4
$V_{\max}$ (C3Gr)	42.	8.4	$E_{K_c}$	59 356.	2967.8
$V_{\max}$ (C4Gr)	8.	1.6	$E_k$	50 967.	2548.35
$V_{\max}$ (Tund)	20.	4.	$\alpha_q$	0.28	0.014
$V_{\max}$ (Wetl)	20.	4.	$\alpha_i$	0.04	0.002
$V_{\max}$ (Crop)	117.	23.4	$K_C$	460.	23.
$a_{J,V}$ (TrEv)*	1.96	0.098	$K_o$	330.	16.5
$a_{J,V}$ (TrDec)*	1.99	0.0995	$a_{\Gamma,T}$ *	1.7	0.085
$a_{J,V}$ (TmpEv)*	2.00	0.1	$\beta$ (TrEv)	1	0.25
$a_{J,V}$ (TmpDec)*	2.00	0.1	$\beta$ (TrDec)	1	0.25
$a_{J,V}$ (EvCn)*	1.79	0.0895	$\beta$ (TmpEv)	1	0.25
$a_{J,V}$ (DecCn)*	1.79	0.0895	$\beta$ (TmpDec)	1	0.25
$a_{J,V}$ (EvShr)*	1.96	0.098	$\beta$ (EvCn)	1	0.25
$a_{J,V}$ (DecShr)*	1.66	0.083	$\beta$ (DecCn)	1	0.25
$a_{J,V}$ (C3Gr)*	1.90	0.095	$\beta$ (EvShr)	1	0.25
$a_{J,V}$ (C4Gr)*	140.	28.	$\beta$ (DecShr)	1	0.25
$a_{J,V}$ (Tund)*	1.85	0.0925	$\beta$ (C3Gr)	1	0.25
$a_{J,V}$ (Wetl)*	1.85	0.0925	$\beta$ (C4Gr)	1	0.25
$a_{J,V}$ (Crop)*	1.88	0.094	$\beta$ (Tund)	1	0.25
$f_{R_{\text{leaf}}}$	0.4	0.1	$\beta$ (Wetl)	1	0.25
$f_{R_{\text{growth}}}$	1.25	0.0625	$\beta$ (crop)	1	0.25

ecosystem productivity (NEP) is derived using conventional formulations for the time variation of soil respiration and a parameterization of storage efficiency to set the overall magnitude (Rayner et al., 2005; see Eqs. 17–22). 56 parameters affect the photosynthesis scheme and both the autotrophic and heterotrophic respiration schemes. These parameters are of two kinds: 3 parameters are PFT-specific (i.e., 39 parameters) and 17 are global parameters. There are 35, 3, and 18 parameters related to GPP, autotrophic respiration, and heterotrophic respiration, respectively (Table 1).

### 2.3 The PYVAR system

The PYVAR system (Chevallier et al., 2005) is a generic Bayesian optimization system used for global and regional

inversions of tracer fluxes. It can be interfaced to several atmospheric transport models. In this case we use the global atmospheric transport model LMDz (Hourdin et al., 2006). PYVAR can ingest various sources of measurements such as surface flask samples and continuous CO<sub>2</sub> concentrations (e.g., Chevallier et al., 2010) and satellite CO<sub>2</sub> data (Chevallier et al., 2007). The PYVAR system also allows for interpolating simulated concentrations to the locations of the stations of the observing network.

### 2.4 Combining CCDAS and PYVAR

In our case we do not use the optimization capabilities of PYVAR. For our error analysis, we require the sensitivity of the observations to the model parameters. For concentration

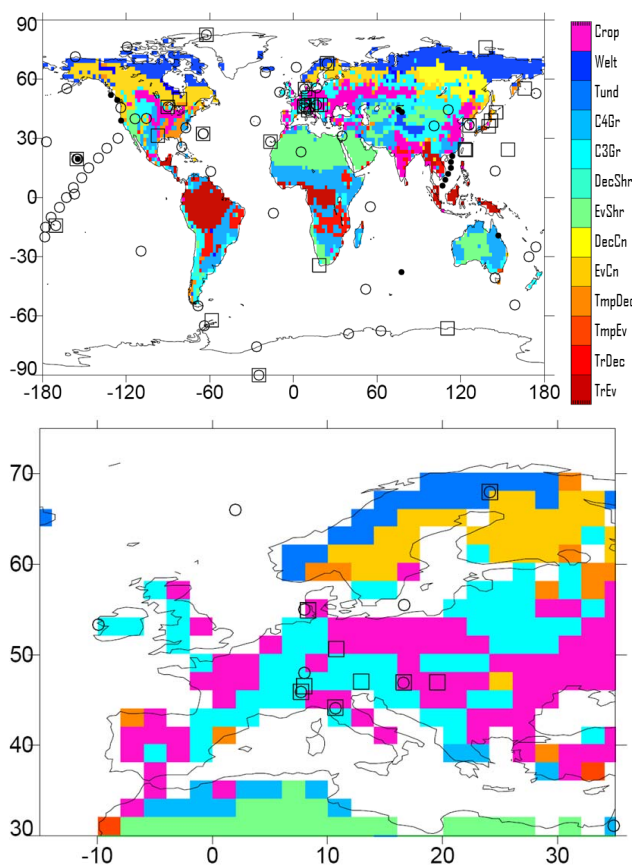


**Fig. 2.** The networks of CO<sub>2</sub> concentration measurements together with the spatial coverage of the 13 plant functional types (PFT) of BETHY with zoom over Europe (bottom) are shown. In each BETHY grid cell, only the dominant PFT is shown. Circles are the network stations with monthly CO<sub>2</sub> concentration used by both TM3 (used in  $M_{TM3}$ ) and LMDz (used in  $M_{PYV}$ ,  $PYV$ , and  $PYV_{all}$ ) models. Squares are stations with high frequency CO<sub>2</sub> data that are used only in LMDz (used in  $PYV$  and  $PYV_{all}$ ). Big dots are stations measuring additional monthly data used in LMDz (used in  $PYV_{all}$ ). For details on the definition of the different settings mentioned above, see Sect. 5.1. The label definitions of the PFTs are Crop – crop plant, Wetl – swamp vegetation, Tund – tundra, C4Gr – C4 grass, C3Gr – C3 grass, DecShr – deciduous shrub, EvShr – evergreen shrub, DecCn – deciduous coniferous tree, EvCn – evergreen coniferous tree, TmpDec – temperate broadleaved deciduous tree, TmpEv – temperate broadleaved evergreen tree, TrDec: tropical broadleaved deciduous tree, TrEv – tropical broadleaved evergreen tree.

observations, we obtain these by first calculating the sensitivity of NEP with respect to parameters, then transporting these sensitivities with LMDz via the PYVAR system (see Fig. 1 and Sect. 3.1 for details on the formalism).

### 3 Computation of uncertainty

The formalism used to calculate the uncertainties in the parameters is first defined. Then, the methods used to quantify the sensitivity of the parameters to observations from both CO<sub>2</sub> concentration and flux measurement networks are described.

#### 3.1 CO<sub>2</sub> concentration network

In this study, we investigate the performance of existing or potential measurement networks. To compute the uncertainty in BETHY parameters with such networks, we apply the network design approach described by Kaminski and Rayner (2008) and demonstrated by Kaminski et al. (2010, 2012b): in brief, the parameters we use were optimized by using a Bayesian inference scheme (Enting, 2002; Tarantola, 2005). This inference scheme minimizes a cost function  $J(x)$  representing the negative log likelihood function.  $J(x)$  includes contributions from the model–observation mismatch and the departure of parameter values from their prior estimates and is defined as follows:

$$J(x) = \frac{1}{2} \left[ \sum_{i=1}^n \frac{1}{(\sigma(d_i))^2} (m_i - d_i)^2 + (x - x_0)^T C(x_0)^{-1} (x - x_0) \right] \quad (1)$$

where  $x$  is the parameter vector to be optimized with prior value  $x_0$  with uncertainty covariance  $C(x_0)$ .  $n$  is the number of observations.  $d_i$  are the observed CO<sub>2</sub> concentrations and  $m_i$  the corresponding values simulated by the transport model. The standard deviation  $\sigma(d_i)$  is derived from the quadratic summed uncertainty (here variance) in the terrestrial model (here BETHY), the transport model, and concentration observations. The parameter errors (or uncertainties) as well as the observation errors are uncorrelated in our formulation. We calculate the second derivative or Hessian ( $H$ ) of the cost function with respect to the parameters (e.g., Kaminski and Rayner, 2008; Kaminski et al., 2010). We consider only the contribution of observations to the Hessian  $H$ , referred to as  $H_m$ , and given by

$$H_m = \sum_{i=1}^n \frac{1}{\sigma(d_i)^2} \left[ \left( \frac{dm_i}{dx} \right)^2 + (m_i - d_i) \left( \frac{d^2 m_i}{dx^2} \right) \right], \quad (2)$$

where  $dm/dx$  is the first derivative (Jacobian) of the simulated CO<sub>2</sub> concentration with respect to the parameters  $x$ . If  $m$  is linear, its second derivative is 0 and we have a simple expression for  $H_m$  in terms of the Jacobian. Under these circumstances the covariance (i.e.,  $(dx/dm)^2$ ) is the inverse  $H_m$  and we see that (as noted by Hardt and Scherbaum, 1994) neither the values of the prior parameters nor the observations appear directly in  $H_m$  (Eq. 2). For a nonlinear model such as BETHY, the sensitivities are, of course, dependent on the value of the optimized parameters.

The total derivative  $dm/dx$  can be written as a function of partial derivatives as follows:

$$\frac{dm}{dx} = \frac{\partial m}{\partial f} \cdot \frac{\partial f}{\partial x} = M \frac{\partial f}{\partial x}, \quad (3)$$

where  $f$  stands for NEP.  $M$  represents the derivative of CO<sub>2</sub> concentration  $m$  with respect to  $f$  (i.e.,  $\partial m/\partial f$ ).  $\partial f/\partial x$  represents the sensitivity of  $f$  with respect to the parameter  $x$ .

The Jacobian matrix  $dm/dx$  is computed by chaining the tangent linear (TL) code of BETHY and the TL code of LMDz via the PYVAR system. The TL code of BETHY is generated by the automatic differentiation tool Transformation of Algorithms in Fortran (TAF; Giering and Kaminski, 1998; Kaminski et al., 2003), while the TL code of LMDz has been coded manually by Chevallier et al. (2005). We first compute the quantities  $\partial f/\partial x$  using the TL code of CCDAS and map them onto the LMDz grid. Then, the TL code of LMDz is used to transport these sensitivities to derive  $dm/dx$ , as given in (Eq. 3).

### 3.2 The Flux measurement network

We note again that this is a synthetic data study where, following our assumption of linearity (as shown in the former equation by replacing  $m$  by  $f$ ), we can calculate the constraint on the parameters without the use of actual data. We do need reasonable values for the parameters since these affect the linearization and, as noted earlier, these are taken from the optimized values of Koffi et al. (2012). In fact, around the optimized values, the assumption of linearization is reasonable.

We use the same linearity assumptions as those used for concentrations so that the critical quantity becomes the Jacobian of the fluxes with respect to parameters (i.e.,  $\partial f/\partial x$ ). These are also calculated by the tangent linear mode of TAF and here we have no need of an atmospheric transport model.

### 3.3 Uncertainty reduction

The contribution of the observations to the Hessian, i.e.,  $H_m$  (Eq. 2; with the second derivative equals zero), is used to approximate the inverse of the covariance matrix that quantifies the uncertainty ranges on the parameters. We use the standard deviation obtained from the inverse of  $H_m$  (Eq. 2) to characterize the uncertainty in the parameters. Following, e.g., Kaminski et al. (1999), we quantify the reduction of the uncertainty (hereafter  $U_R$ ) in a selected parameter from its prior as follows:

$$U_R(\%) = 100 \cdot \left( 1 - \frac{\sigma_x}{\sigma_{x0}} \right), \quad (4)$$

where  $\sigma_x$  (derived from Eqs. 2–3) and  $\sigma_{x0}$  (Table 1) are the posterior and prior uncertainties in the parameter  $x$ , respectively.

## 4 Data

### 4.1 CCDAS

The system needs both forcing data to drive BETHY and atmospheric CO<sub>2</sub> concentration data for the assimilation. BETHY is driven by observed monthly climate and radiation data over the period 1979–2001 (Nijssen et al., 2001). In addition, daily values of such data are available for the period 1996–2006. For both the photosynthesis and soil schemes in BETHY, the phenological data, i.e., leaf area index (LAI) and plant available soil moisture  $\omega$  (as a fraction of maximum soil water capacity) are also available for the two above mentioned periods. We assumed atmospheric concentration measurements are available at the 68 stations used by Koffi et al. (2012).

#### 4.1.1 BETHY fluxes

In the standard setup of CCDAS, BETHY is run such that it simulates hourly GPP and NPP for one representative day in a month. In this study, in addition to the standard run, we adapt the BETHY output to calculate for each day of the month. We use hourly sensitivities of modeled quantities to BETHY model parameters for one representative day in a month. To quantify the contribution of hourly flux measurements to the reduction of uncertainties in parameters, we used hourly NPPs as a proxy of NEPs. The storage efficiency scheme is not appropriate for calculating hourly heterotrophic respiration. We assume that the magnitude of the diurnal cycle (noted by Knorr and Kattge (2005) as the key observable from hourly flux measurements) is driven by NPP, not heterotrophic respiration. Hence, when considering the flux measurement network, only the thirty-eight parameters relevant for NPP are first analyzed (Table 1). There is no clear algorithm for assigning uncertainties to flux data in CCDAS since it varies widely with conditions (Hagen et al., 2006) and depends on the capability of the model itself (Chevallier et al., 2012). However, random flux measurement uncertainty, expressed as a standard deviation, was found to vary with the flux magnitude (Richardson and Hollinger, 2005; Richardson et al., 2008; Lasslop et al., 2008). The authors showed that the error distribution in NEE (net ecosystem exchange) is leptokurtic (i.e., the peaks result from the data being highly concentrated around the mean) and it is described better by a double exponential (Laplace) than a Gaussian distribution. However, when grouping the data according to the flux magnitude, Lasslop et al. (2008) found that high flux magnitudes follow a Gaussian distribution and that the leptokurtic error distribution found for all the data is largely due to low flux magnitudes. In addition, the parameters in the error distributions are dependent on the observational site. In this study, we therefore choose a conservative value of 25 % of the hourly observed quantity. Note that this will translate into much larger percentage errors in diurnal and annual

sums (where fluxes partially cancel but errors do not). Thus, the uncertainties in BETHY hourly NPP observations are assumed to be equal to 25 % of the corresponding NPP values. To test the sensitivity of flux measurements to the parameters strongly related to NEP, we use a “pseudo” hourly NEP computed by dividing the daily heterotrophic respiration into 24 equal-sized hourly fluxes and subtract these fluxes from the hourly NPP, as performed in Kaminski et al. (2012b). As for the NPP observations, we assume that the measurement uncertainties in these NEP are equal to 25 % of the corresponding NPP values. When NPP equals zero, we consider larger uncertainties to be 25 % of the maximum of the NPP, which is obtained from all the grid cells of BETHY and over the selected period.

#### 4.1.2 Prior values of the parameters and uncertainties

The uncertainties in prior parameters of BETHY are those of Koffi et al. (2012). For bio-physical parameters (e.g., the carboxylation capacity of the leaf,  $V_{\max}$ ); the prior values are taken from literature summarized in Knorr (2000). For other parameters such as the beta storage efficiency ( $\beta$ ) relevant for carbon balance NEP, the uncertainties are assumed to be large since there is little knowledge of these parameters (Table 1). Finally, prior information not only includes results of previous studies but also knowledge of the physical limits of the parameters. For example, many parameters are physically limited to positive values. A log-normal PDF was considered for these bounded parameters while a Gaussian PDF was applied to those parameters that do not have such critical threshold values (marked by an asterisk in Table 1; Koffi et al., 2012).

#### 4.1.3 Transport model and CO<sub>2</sub> concentrations

For the tracer transport, we use the precomputed transport Jacobians of the TM3 model (Heimann and Körner, 2003). TM3 has a resolution of 4 degrees latitude by 5 degrees longitude with 19 levels. It uses NCEP (National Centers for Environmental Prediction) meteorological fields as input. We use the monthly averaged precomputed transport Jacobians of Roedenbeck et al. (2003) over the 1979–2001 period with meteorological forcing that varied each year. The error in the TM3 model is considered in the observation error budget, as given hereafter.

For CCDAS, we use monthly mean atmospheric CO<sub>2</sub> concentration data from 68 sites from the GLOBALVIEW database [GLOBALVIEW-CO<sub>2</sub>, 2004] and some additional CO<sub>2</sub> measurement sites for which the TM3 Jacobians are available. The uncertainties in these data include those from models (BETHY and transport) and measurement errors and range from 0.50 ppm to about 5.0 ppm (see Table A2 in the Supplement), as described in Koffi et al. (2012).

## 4.2 PYVAR

The PYVAR system allows CO<sub>2</sub> fluxes to be estimated at relatively high temporal resolution (up to 8 three-hour time windows per day). The fluxes and CO<sub>2</sub> concentrations are linked in the PYVAR system by the LMDz model (Hourdin et al., 2006). LMDz has 19 levels and a horizontal resolution of 2.5° in latitude and 3.75° in longitude. LMD<sub>Z</sub> is an on-line model, i.e., it generates its dynamics internally along with tracer transport. To ensure realistic simulation of actual meteorological conditions the model is nudged towards ECMWF (European Centre for Medium-Range Weather Forecasts) re-analyses. We then archive mass fluxes and run the model offline. The ECMWF reanalyses for 1989–2006 are used.

To represent the CO<sub>2</sub> concentration measurement network, we use the same data as Chevallier et al. (2010). These data come from three large data bases: The NOAA Earth System Laboratory (ESRL) archive, the CarboEurope IP project, and the World Data Centre for Greenhouse Gases (WD-CGG) of the World Meteorological Organization (WMO) Global Atmospheric Watch Programme. The three databases include both in situ measurements made by automated quasi-continuous analyzers and air samples collected in flasks and later analyzed at central facilities. The data treatments are fully discussed in Chevallier et al. (2010). Data collected from up to 104 stations are considered (see Fig. 2 for locations of the stations). The errors in the LMDz model are included in the observational error following Tarantola (2005). The treatment of these errors follows that of Chevallier et al. (2010). Values range from 0.37 ppm to about 30 ppm, depending on the temporal resolution of the observations (see Table A2 in the Supplement). The large values for some observations compensate for the absence of explicit correlations in the assigned transport model errors for temporally dense data. There is also a contribution from model error in BETHY. For concentrations we assume this is small compared to transport error while for fluxes we treat it by assigning errors of 25 %, much larger than the observational error (see Sect. 4.1.1). Sensitivity studies for the uncertainty in concentrations showed little sensitivity of most posterior parameter values to increasing the observational error in concentrations by 2 ppm.

#### 4.3 Combination of CCDAS and PYVAR data

CCDAS provides monthly or daily NEP and their sensitivities with respect to BETHY parameters to the PYVAR system (see Fig. 1). To use high frequency observations of CO<sub>2</sub> concentrations, PYVAR divides the day into 8 three-hour time windows in which the flux is constant. When using monthly fluxes from CCDAS within PYVAR, the value of the flux for a month is considered representative for the days of the month and for each of the 8 time windows of a day. For daily NEP, the value of the flux for a day is considered

**Table 2.** Model/data configurations for CO<sub>2</sub> concentration networks are shown. For  $M_{TM3}$ ,  $M_{PYV}$ , PYV, and PYV<sub>all</sub>, the period of the study is 1989–2001. For the configurations MM<sub>PYV</sub>, DM<sub>PYV</sub>, and DD<sub>PYV</sub>, we consider single years over the 1998–2005 period. The minimum and maximum numbers of stations derived for each year over this 1998–2005 period are given.

Model/data configurations	Temporal resolutions of forcing data (meteo and pheno) for BETHY		Temporal resolutions of inferred BETHY fluxes		Temporal resolutions of CO <sub>2</sub> concentrations		Number of stations
	Monthly	Daily	Monthly	Daily	Monthly	Continuous	
$M_{TM3}$	x		x		x		62
$M_{PYV}$	x		x		x		62
PYV	x		x		x	x	62
PYV <sub>all</sub>	x		x		x	x	104
MM <sub>PYV</sub>	x		x		x	x	72–88
DM <sub>PYV</sub>		x	x		x	x	72–88
DD <sub>PYV</sub>		x		x	x	x	72–88

representative for each of the 8 time windows of PYVAR. The used Jacobians correspond to full-day averages.

## 5 Experimental setup

The different configurations of model/data used to study the sensitivity of the parameters to (i) high frequency observations of CO<sub>2</sub> concentrations and (ii) temporal resolution of meteorological and phenological data used to force BETHY are first defined. Then, the configurations relevant for flux measurement network are given.

### 5.1 Configurations using observing network of CO<sub>2</sub> concentration

To test the sensitivity of the parameters to high frequency CO<sub>2</sub> concentration data, we first use BETHY monthly NEP over the period 1989–2001 to compute various versions of the Jacobian relating parameters to atmospheric concentrations (see Eq. 3). The following configurations, which are summarized in Table 2 and Fig. 1, are considered:

- $M_{TM3}$ : monthly CO<sub>2</sub> observations at 62 sites (i.e., the number of stations that are common for both CCDAS and PYVAR) over the period of 1989–2001 by using Jacobians of TM3.
- PYV: the PYVAR system is used for the 62 common sites and for the period 1989–2001. Only the monthly NEP from CCDAS is considered. The treatment of these fluxes in PYVAR is given in Sect. 4.3. We use continuous CO<sub>2</sub> concentrations when available at these stations. For noncontinuous sites, the data frequency is weekly or biweekly.
- $M_{PYV}$ : the results obtained by averaging PYV data monthly and for which data from  $M_{TM3}$  exist. This is the closest comparable case to  $M_{TM3}$ .

- PYV<sub>all</sub>: as for PYV configuration, but for all the stations used in Chevallier et al. (2010). In total, we consider 104 stations over the period 1989–2001.

The differences between  $M_{TM3}$  and  $M_{PYV}$  configurations give information on the sensitivity of parameters to the transport models while  $M_{PYV}$ , PYV, and PYV<sub>all</sub> give the sensitivity of the parameters to number, frequency, and type of observations. The observing networks of CO<sub>2</sub> concentrations for the configurations defined above are shown in Fig. 2.

Here we summarize the characteristics of flask and continuous measurements for the stations used for CO<sub>2</sub> concentrations:

- 77 flask measurements, among which 62 are common between CCDAS (i.e.,  $M_{TM3}$ ) and PYVAR (i.e.,  $M_{PYV}$ ). The remaining 15 sites are only for PYVAR (PYV and PYV<sub>all</sub>). We used full-day averages of flask measurements. The uncertainties in these measurements, including model errors, are summarized in Table A2 of the Supplement.
- 27 sites with continuous measurements used only by PYVAR, among which 9 sites also have flask measurements. We averaged data from continuous sites into 3 h windows in the PYVAR system.
- The measurement uncertainties, which here represent both the model and observation uncertainties, are provided in the supplementary material (Table A2) for all the sites used in this study.

### 5.2 Configurations using daily fluxes

To test the sensitivity of the parameters to the temporal resolution of the meteorological and phenological data used to force BETHY, and hence to the temporal resolution of BETHY fluxes, we use the following configurations, which are also summarized in Table 2 and Fig. 1:

**Table 3.** Characteristics of the flux measurement networks are given. BETHY-PFT is a network composed of 13 pixels of BETHY with dominant PFTs. The fractions of these PFTs are indicated. BETHY-FLUXNET is the network based on the stations of the international FLUXNET network. The dominant PFTs of BETHY at these stations are indicated.

PFT acronym	BETHY-PFT	BETHY-FLUXNET	
	Fractions of coverage of the dominant PFT	Number of pixels (or stations) per PFT	Maximum of the fractions of coverage of the dominant PFT
TrEv	0.9	14	0.9
TrDec	1.00	3	1.00
TmpEv	0.92	3	0.92
TmpDec	1.00	14	1.00
EvCn	1.00	18	1.00
DecCn	0.517	1	0.517
EvShr	1.00	2	1.00
DecShr	0.517	1	0.517
C3Gr	1.00	44	1.00
C4Gr	0.867	28	0.517
Tund	1.00	9	1.00
Wetl	1.00	1	0.867
Crop	1.00	35	1.00

- MM<sub>PYV</sub>: both monthly meteorological and phenological data are used to force BETHY. The simulated monthly fluxes by BETHY are considered.
- DM<sub>PYV</sub>: both daily meteorological and phenological data are used to force BETHY. Daily fluxes are calculated from BETHY, but monthly mean values from these daily fluxes are considered. Comparison with MM<sub>PYV</sub> tests the sensitivity to the assumption of a single representative day made in BETHY.
- DD<sub>PYV</sub>: both daily meteorological and phenological data are used to force BETHY. Daily fluxes computed by BETHY are considered.
- BETHY-PFT: we use 13 sites that cover the 13 PFTs of the BETHY model. The stations are selected on the basis of the dominant PFTs of BETHY. Table 3 gives the percentages of coverage of the 13 PFTs over their corresponding BETHY grid cell (Fig. 3). Note that this network is constructed similarly to the 9 PFT networks over Europe used in Kaminski et al. (2012b), except that Kaminski et al. (2012b) assigned 100 % coverage of the dominant PFTs.
- BETHY-FLUXNET: we consider a network based on both the international FLUXNET network (Baldocchi, 2003 and Papale et al., 2006; see the dedicated website <http://www.fluxnet.ornl.gov>) and three BETHY PFTs. We first consider the BETHY grid cells that cover at least one site of the FLUXNET network. We obtain a network with 172 BETHY pixels. For each of these grid cells, we consider the dominant PFT. When doing so, three PFTs of BETHY are missing. They are deciduous coniferous (DecCn), deciduous shrub (DecShr), and swamp vegetation (Wetl). Kaminski et al. (2012b) has shown that as soon as a PFT is left unsampled by the flux network, it dominates the uncertainty in area-integrated flux. Thus, we have added three hypothetical sites to get a network with 175 sites (or BETHY grid cells) (Table 3). It is worth noting that some PFTs of BETHY are overrepresented in the BETHY-FLUXNET network (Table 3). For example, the C4 grass PFT is represented by 28 grid cells of BETHY (or stations), while only 1 grid cell is used for swamp vegetation (Wetl). Also, for some PFTs, the percentages of coverage over their relevant BETHY pixels are low (Table 3). The networks relevant to BETHY-PFT

The differences between MM<sub>PYV</sub> and DM<sub>PYV</sub> give information on the sensitivity of the parameters to the temporal resolution of the meteorological and phenological data. The configurations MM<sub>PYV</sub> and DD<sub>PYV</sub> probe the sensitivity of the parameters to the temporal resolution of BETHY fluxes. For these three configurations, all the available stations of the observing network of CO<sub>2</sub> concentrations that can be handled by the PYVAR system are used. Results of MM<sub>PYV</sub>, DM<sub>PYV</sub>, and DD<sub>PYV</sub> are derived for several single years drawn from the period 1996–2006.

### 5.3 Configurations using the flux measurement network

In our model, a flux measurement samples the flux over a particular grid cell. The sensitivities of flux measurements to the model parameters are computed as described in Sect. 3.2. We design two configurations for two potential networks of flux measurements. We use BETHY-generated hourly NPP and NEP as a proxy of flux measurements (Fig. 1):

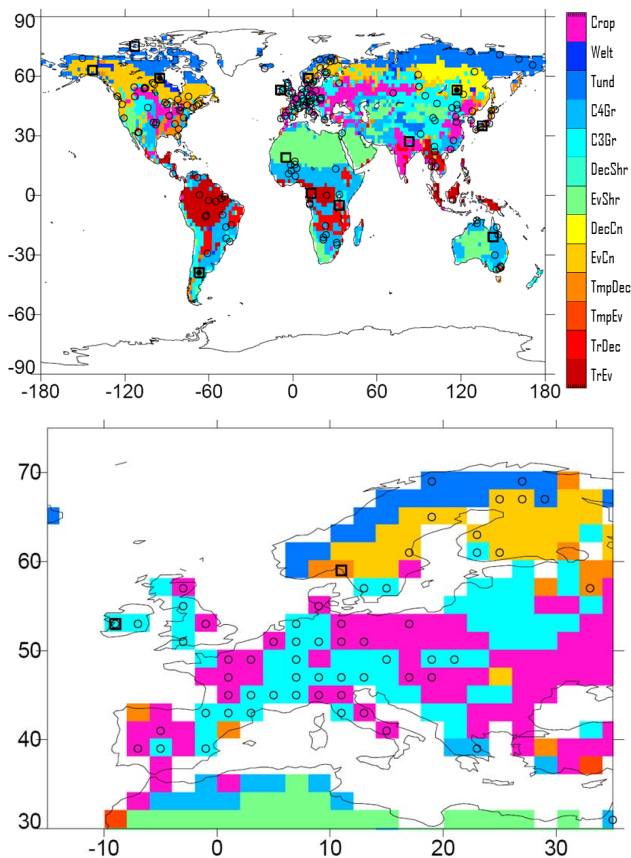


**Fig. 3.** The networks of flux measurements we use (top) with a zoom over Europe (bottom) are shown. Rectangle symbols are stations of the network based on the 13 PFTs of BETHY (called BETHY-PFT). Circles are locations of FLUXNET stations. The big dots correspond to locations of 3 PFTs (6, 8, and 12) of BETHY used to complete the FLUXNET stations. In total, there are 175 stations (dot and circle symbols) representing our large flux measurement network (i.e., BETHY-FLUXNET). See Fig. 2 for the definition of the acronyms of the PFTs.

and BETHY-FLUXNET configurations are shown in Fig. 3.

Since we use BETHY fluxes as a proxy of FLUXNET flux measurements, we have compared BETHY hourly fluxes to observed ones obtained from some selected FLUXNET sites located around the world. Results show that BETHY fluxes are in reasonably good agreement with the observations (see the Supplement provided for this paper).

## 6 Results

### 6.1 Uncertainty reduction with high frequency and continuous CO<sub>2</sub> concentrations

Figure 4 shows the reduction of the uncertainties ( $U_R$ ) for the 56 studied parameters of BETHY (see Table 1 for the defi-

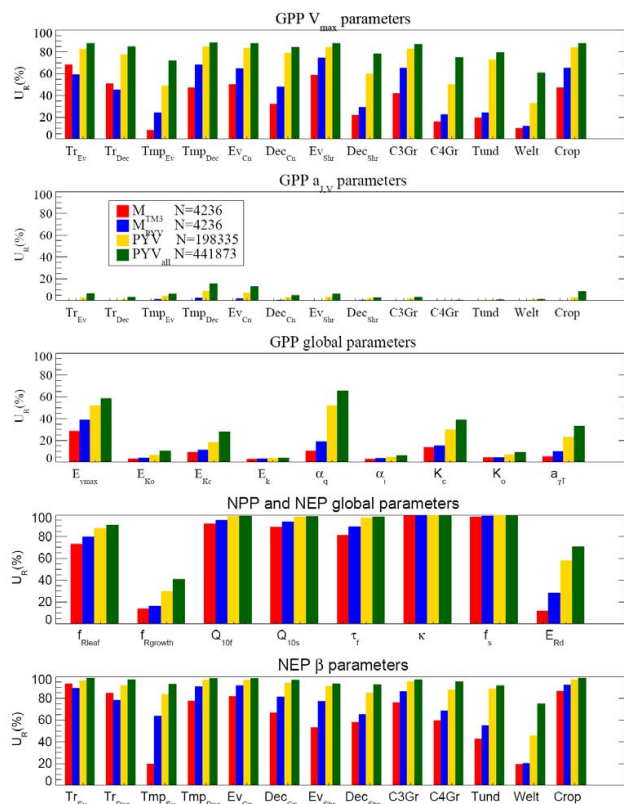


**Fig. 4.** Uncertainty reduction ( $U_R$ ) for the 56 parameters of BETHY. Results from  $M_{TM3}$ ,  $M_{PYV}$ ,  $PYV$ , and  $PYV_{all}$  configurations that cover 1989–2001 period are shown. The number of observations  $N$  for each configuration is indicated. The model/data configurations  $M_{TM3}$ ,  $M_{PYV}$ ,  $PYV$ , and  $PYV_{all}$  are defined in Sect. 5.1 and Table 2. See Fig. 2 for the definition of the acronyms of the PFTs and Table 1 for the prior values of the parameters.

nition of the parameters) when considering  $M_{TM3}$ ,  $M_{PYV}$ , and  $PYV$ , and  $PYV_{all}$  configurations (see Sect. 5.1). We have 4236 pairs of observations for both  $M_{TM3}$  and  $M_{PYV}$ , 198 335 observations for  $PYV$ , and 441 873 observations for  $PYV_{all}$ , respectively. Overall, the uncertainty reductions in the parameters are not significantly sensitive to the transport models. Similar  $U_R$  values are found between  $M_{TM3}$  (TM3 model) and  $M_{PYV}$  (LMDz model). The differences in  $U_R$  between  $M_{TM3}$  and  $M_{PYV}$  are less than 25 % for 55 of the 56 parameters (Fig. 4). The largest difference (44 %) is obtained for NEP parameter  $\beta$  for the temperate evergreen forest (Tmpev). We also investigated the differences between  $M_{TM3}$  and  $M_{PYV}$  (not shown). We have run the  $M_{PYV}$  setup with the uncertainty from the  $M_{TM3}$  setup. On average, the uncertainties assigned to the concentrations when using  $M_{TM3}$  setup are 1.8 lower than those for  $M_{PYV}$  (see Table A2 in the Supplement). Compared to the default  $M_{PYV}$  setup, this increases the uncertainty reduction for all parameters.

As expected, the uncertainties in the parameters are more strongly reduced as the number of observations increases but

the reduction becomes relatively small between two large sets of observations. As an example, for  $V_{\max}$  of the tropical evergreen forest,  $U_R$  values are 59 % and 81 % when using 4326 ( $M_{\text{PYV}}$ ) and 198 335 (PYV) observations, respectively. It is only 88 % from 441 873 observations. When considering the PYV<sub>all</sub> configuration (which represents the largest number of observations used), the largest uncertainty reductions (> 90 %) are obtained for almost all the parameters related to carbon balance NEP (i.e.,  $\beta$ ) and to soil respiration (i.e.,  $Q_{10f}$ ,  $Q_{10s}$ ,  $\tau_f$ ,  $\kappa$ ,  $f_s$ ). The smallest reduction (75 %) is found for the  $\beta$  parameter relevant for swamp vegetation (Wetl PFT). These results agree with those reported in Ziehn et al. (2011), who investigated the sensitivity of the uncertainty reductions in BETHY parameters to the spatial variations of the PFTs. The authors also found large uncertainty reductions in the parameters, but less than the reductions obtained when considering original PFTs.

For the PYV<sub>all</sub> configuration, the uncertainties in  $E_{\text{Rd}}$  and  $f_{\text{R,leaf}}$  (i.e., leaf respiration) parameters relevant for NPP are reduced by 60 % and 90 % from their prior values, respectively (Fig. 4). Only a weak reduction is obtained for the parameter  $f_{\text{R,growth}}$  relevant for the growth respiration of the plant (about 40 %). Significant reductions (between 60 % and 90 %) are found for the  $V_{\max}$  parameters, with the largest reduction being for  $V_{\max}$  for temperate deciduous (TmpDec) forest. The smallest reduction is again obtained for swamp vegetation (i.e., Wetl PFT). We obtain relatively small uncertainty reductions for the parameters  $a_{J,V}$  (< 15 %). Note that  $a_{J,V}$  is the slope of the linear relationship between the maximum electron transport and  $V_{\max}$  at 25 °C. The uncertainties are also weakly reduced (< 40 %) for almost all the global parameters relevant for photosynthesis (i.e.,  $E_{K_0}$ ,  $E_K$ ,  $\sigma_{i25}$ ,  $K_0$ ). Among these global parameters, only the uncertainties in both  $E_{V_{\max}}$  and  $\alpha_q$  parameters are significantly reduced (about 60 %).

We find that uncertainty reduction saturates for large numbers of observations (not shown). As discussed in Kaminski et al. (2012a, b), we can understand the saturation of the information provided by observations by considering the eigenvectors of the Hessian. These describe particular directions in parameter space; the related eigenvalues are a measure of the information content in that direction. Increasing the number of observations may well improve the information content in a particular direction but not necessarily constrain new directions in parameter space. Eventually the uncertainty in a particular direction approaches zero and the uncertainty in a parameter is determined by its projection onto the subspace spanned by the well-constrained directions. With 56 parameters we have 56 available directions in parameter space. An analysis of the eigenvalues for our different cases shows the observations constrain at most 40 of these directions. Observing these directions better will not provide much more information; only new types of observations will constrain the remaining directions. This is supported by research at smaller scales using ecosystem models

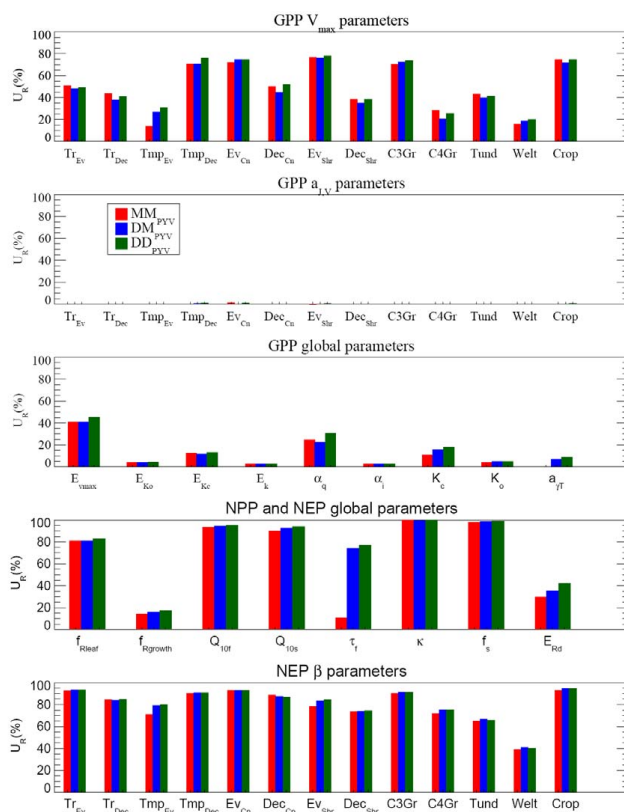


**Fig. 5.** As for Fig. 4, but for the model/data configurations  $MM_{\text{PYV}}$ ,  $DM_{\text{PYV}}$ ,  $DD_{\text{PYV}}$  and for the year 2000. The number of observations for the year 2000 is 30 332 and this for each of the configurations.

(e.g., Williams et al., 2009; Moore et al., 2008; Zobitz et al., 2008; Richardson et al., 2010).

## 6.2 Uncertainty reduction with daily fluxes

Our initial hypothesis was that the response of daily fluxes to variations in forcing would contain information about the model parameters and would, in turn, be visible in daily measurements of CO<sub>2</sub> concentration. We investigate this using the  $MM_{\text{PYV}}$ ,  $DM_{\text{PYV}}$ , and  $DD_{\text{PYV}}$  configurations. Figure 5 shows  $U_R$  for the year 2000. The number of observations used is 30 332. Overall,  $U_R$  for all three cases are roughly comparable. This surprising result comes despite the well-documented capability of high-frequency observations to resolve details of flux distributions (Law et al., 2003). It raises the question whether this is a fundamental limit or a function of the placement of current stations. Following Koffi et al. (2012), we investigate this by calculating global fields of the sensitivity of concentration to parameters rather than the Jacobians at stations. We simulate the sensitivity of surface CO<sub>2</sub> concentrations to parameters by using the LMDz model. We use the sensitivities of NEP with respect to  $V_{\max}$  for tropical evergreen and temperate deciduous forests, respectively.

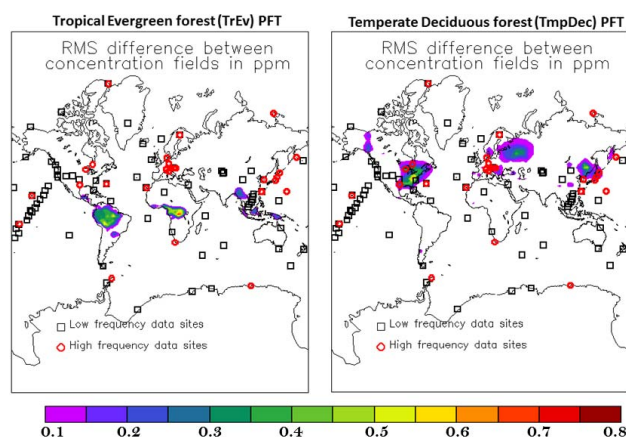


**Fig. 6.** Root mean square (RMS) deviation (ppm) between surface sensitivities of CO<sub>2</sub> concentration to parameter obtained from the sensitivities of monthly and daily NEP of BETHY with respect to the parameters  $V_{\max}$  for tropical evergreen forest (TrEv) (left) and temperate deciduous forest (TmpDec) (right) are shown, respectively. Simulations are performed through the global transport model LMDz. The values are annual means (see Sect. 6.2 for more details).

Sensitivities from the cases MM<sub>PYV</sub> and DD<sub>PYV</sub> are considered. We run the transport model LMDz for 3 yr using the two NEP sensitivities obtained for year 2000 as inputs. We then analyze the surface fields of the last year of LMDz simulations. The differences between the two simulations are quantified by the root mean square difference (rmsd) computed both in space and time (Fig. 6). For both cases, the differences between the daily and monthly cases are restricted to the regions of the relevant PFTs. Thus, the impact of considering the daily flux responses to these two parameters does not travel far enough to be observed by the sparse network.

### 6.3 Interannual variability of uncertainties in parameters

Figure 7 shows  $U_R$  for the years 1998, 2000, 2001, 2003 and 2005. These years were chosen to represent the interannual variability in the forcing. We do not find large differences in uncertainty reductions (less than 19 %) between the different years. The relatively small differences between the selected years occur despite large differences in the density of observations. As an example, the year 1998 exhibits similar uncertainty reductions as the year 2005 for  $V_{\max}$  relevant for the tropical evergreen forest (TrEv), but 2005 has about 2.4 times the number of observations of 1998 (Fig. 7), with mean uncertainty 1.4 times as large.

### 6.4 Uncertainty reduction with flux measurements

Figure 8 shows  $U_R$  values obtained when using NPP flux measurements for the year 2000 and for the two

cases BETHY-PFT and BETHY-FLUXNET. We have 3744 and 50 400 observations for BETHY-PFT and BETHY-FLUXNET, respectively. There are dramatic uncertainty reductions for all the GPP  $V_{\max}$  parameters and the parameters  $f_{R,\text{leaf}}$  and  $f_{R,\text{growth}}$  relevant to NPP. Except for the tundra PFT, BETHY-PFT produces uncertainty reductions in  $V_{\max}$  of more than 80 %. This is more effective than the DD<sub>PYV</sub> case (i.e., CO<sub>2</sub> concentration network with daily BETHY fluxes). Note that the number of observations used, e.g., for BETHY-PFT, is only 12 % of that of DD<sub>PYV</sub>. This confirms the result of Kaminski et al. (2012b), who found uncertainty reductions of over 99 % in simulated NEP and NPP over Europe with only 9 flux sites. Consequently, these results demonstrate the potential of high frequency flux measurements in reducing the uncertainties in  $V_{\max}$  parameters. When using a larger number of flux measurements allowed by the BETHY-FLUXNET configuration, very large uncertainty reductions are obtained for all the parameters  $V_{\max}$  of GPP and the three parameters of NPP (between 85 % and 98 %), as shown in Fig. 8.

In contrast to observations of CO<sub>2</sub> concentrations, flux data significantly constrains other parameters such as the  $a_{J,V}$  (PFT dependent) and global parameters related to photosynthesis (i.e., to GPP). As expected, the constraint increases with the number of measurements, hence  $U_R$  for BETHY-FLUXNET is highly variable. For the C4 plant,  $a_{J,V}$  is not sensitive to flux measurements (Fig. 8). Indeed, we do not find any difference between BETHY-PFT and BETHY-FLUXNET configurations, but BETHY-FLUXNET uses 28 times the number of observations of BETHY-PFT. This is due to the fact that the Jacobians are close to zero for this parameter.  $E_{V_{\max}}$ , which appears in the descriptions of both C3 and C4 photosynthesis, shows  $U_R$  of 91 % while most parameters that affect C3 photosynthesis only yield 48–85 %. For C4 vegetation, the parameter  $E_k$  does not show any  $U_R$ , suggesting that  $V_{\max}$  limitation is not active.

As expected, eddy flux measurements allow us to greatly reduce the uncertainties in the parameters related to the carbon balance NEP (i.e.,  $\beta$ ) (Fig. 9). Moreover, with NEP measurements, uncertainty reductions for some  $a_{J,V}$  parameters related to photosynthesis become larger (e.g., C4 grass and Wetl) (Figs. 7, 8, and 9).

As might be expected with the stronger constraint afforded by flux measurements, combining flux and concentration measurements does not improve much on the flux-only case (Figs. 7, 8, and 9).

The data uncertainty in fluxes is dominated by model error. We have carried out a sensitivity study (not shown) in which we used as uncertainties in NEP 75 % of their corresponding NPP values (see Sect. 4.1.1 for detail on the uncertainty assignment). In this case, the smaller flux network BETHY-PFT still yielded reductions in parameter uncertainties larger than with concentration measurements alone, but here the differences were not so clear.

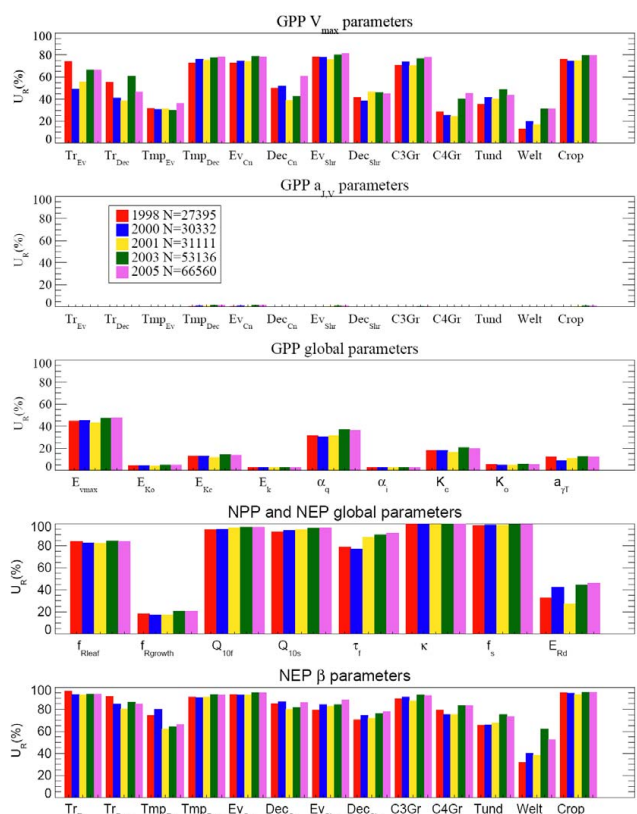


**Fig. 7.** Uncertainty reductions ( $U_R$ ) for various years when using daily meteorological and phenological data to force BETHY are shown. BETHY modeled daily fluxes are considered to compute the uncertainties (i.e., DD<sub>PYV</sub> configuration). The number of observations  $N$  for each year is indicated. See Fig. 2 for the definition of the acronyms of the PFTs and Table 1 for the prior values of the parameters.

### 6.5 Sensitivities of observations to parameters

Finally, we have investigated the sensitivities of both the CO<sub>2</sub> concentration (Eq. 3) and flux with respect to each of the 56 studied parameters (not shown). For CO<sub>2</sub> concentrations, as expected the largest sensitivities are found for parameters related to soil respiration and carbon balance NEP. The largest sensitivity is found for the parameter  $f_s$ , which describes the fraction of decomposition from the short-lived litter pool that goes to the long-lived soil carbon pool. The weakest sensitivity is found for the parameter  $E_k$  relevant for the PEP case (i.e., the initial CO<sub>2</sub> fixing enzyme in C4 plants). Concerning the flux measurements (here NPP), the largest sensitivities are found for parameters relevant for NPP and some parameters  $V_{\max}$  of GPP. The largest sensitivity is obtained for the parameter  $f_{R\text{leaf}}$ , the fraction of GPP used for the maintenance respiration of the plant. Again, the weakest sensitivity is for  $E_k$ . See Rayner et al. (2005) and Koffi et al. (2012) for details of the parameters and the physical quantities they affect.

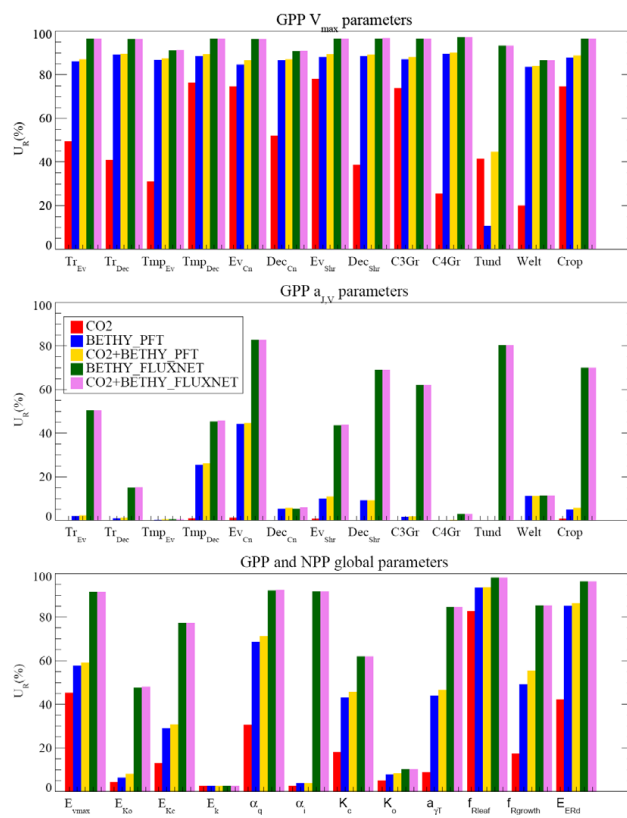


**Fig. 8.** Uncertainty reductions ( $U_R$ ) for the parameters of BETHY relevant to GPP ( $V_{\max}$ ,  $a_{J,V}$ ,  $E_{V_{\max}}$ ,  $E_{K_o}$ ,  $E_{K_c}$ ,  $E_k$ ,  $\alpha_q$ ,  $\alpha_i$ ,  $K_c$ ,  $K_o$ ,  $a_{JT}$ ) and NPP ( $f_{R\text{leaf}}$ ,  $f_{R\text{growth}}$ ,  $E_{R_d}$ ) are shown. The parameters are defined in Table 1. Results for the year 2000 and from the network of CO<sub>2</sub> concentration (i.e., CO<sub>2</sub>) derived from DD<sub>PYV</sub> configuration (which uses daily fluxes from BETHY within the PYVAR system; see Sect. 5.1 for details) are shown. The model/data configurations BETHY-PFT and BETHY-FLUXNET are defined in Sect. 5.2 and Table 3. The number of observations used are 30 332 (CO<sub>2</sub>), 3744 (BETHY-PFT), and 50 400 (BETHY-FLUXNET). See Fig. 2 for the definition of acronyms of the PFTs and Table 1 for the prior values of the parameters.

## 7 Discussion

The above results raise two questions. Firstly, why are the flux measurements so much more effective as a constraint in the CCDAS? Atmospheric concentrations, in the inverse method we use here, are themselves an observation of integrated flux. Yet they are far less effective as a constraint on process parameters than the fluxes themselves. There are two likely reasons for this, both to do with the integrating action of atmospheric transport. Firstly, each concentration observation integrates information from many flux pixels. This means they average out local variations in forcing that would otherwise provide information on the response of processes. This effect is reduced for seasonal and interannual forcing where climate anomalies are usually spatially coherent but we still lose much small-scale information. The other reason

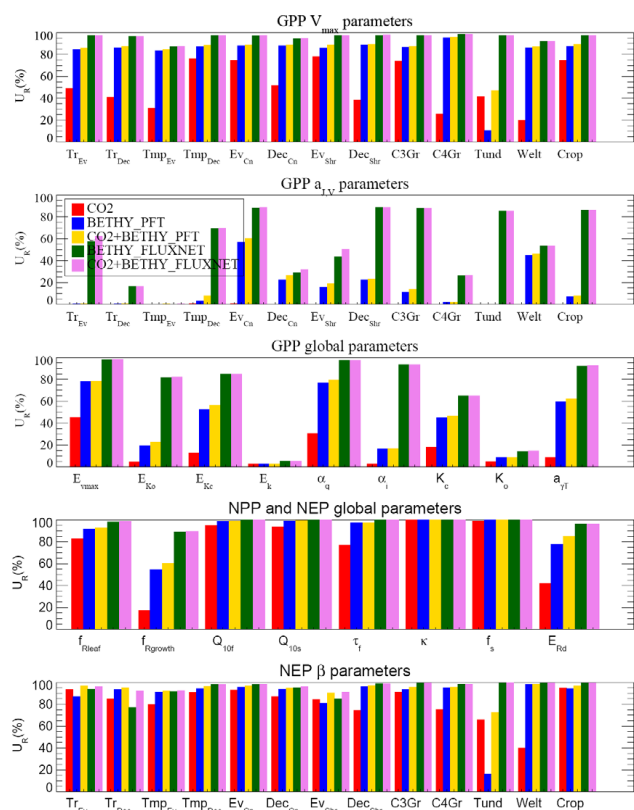


**Fig. 9.** As for Fig. 8, but considering NEP flux measurements and then for all the 56 studied parameters of BETHY. See Fig. 2 for the definition of the acronyms of the PFTs and Table 1 for the prior values of the parameters.

has already been mentioned, the spatial confinement of signals from high-frequency flux responses. Part of this problem may be addressed by spatially dense satellite measurements of concentration (Kaminski et al., 2010).

The other point to be drawn from the study is the relative value of flux and concentration measurements within a CC-DAS. If our aim is limited to constraining parameters of biosphere process models, our results alone would argue for a substantial shift of resources from concentration to flux measurements. Of course this is not the only purpose of atmospheric measurements but it is an important one, contributing to the intensification of continental networks in the last decade. A counterpoint to this conclusion is provided by the recent study of Kaminski et al. (2012b). Using different metrics but similar techniques, they also showed a much greater power of flux observations in reducing uncertainty of parameters in CCDAS and resultant calculated fluxes. Their results were, however, highly sensitive to the assumed heterogeneity of the biosphere. As soon as a PFT was left unsampled by the flux network it dominated the uncertainty in area-integrated flux. Since we can never be sure of the true process-level heterogeneity, a combined observing strategy is clearly required.

The study showed large reductions of uncertainty for most BETHY parameters. Throughout our process we noted the dependence of this result on the magnitude of data uncertainties we used and have therefore conducted sensitivity studies where possible to quantify this dependence. It is likely that (unknown) correlations in the model errors significantly dampen the real observation impact. However, model error in BETHY is a contributor to uncertainties in both types of observations, so an underestimate of this contribution will affect both networks. It should therefore have less impact on our conclusion that flux observations are a strong constraint compared to concentration observations. More important here is the conclusion from Ziehn et al. (2011) and Kaminski et al. (2012b), who noted that increased complexity (i.e., regionalization of the PFTs) of the biosphere description both reduced the impact of observations on parameter uncertainty but particularly reduced the impact of flux observations.

This analysis is restricted to only two types of measurements. Other data such as the fluorescence data from the GOSAT satellite (Frankenberg et al., 2011), satellite-derived fAPAR (Knorr et al., 2010; Kaminski et al., 2012a), and leaf level observations (Ziehn et al., 2011) can be used as additional data to constrain the parameters related to GPP and NPP. Also, the inclusion of soil respiration observations should help in constraining the heterotrophic parameters (Richardson et al., 2010).

## 8 Conclusions

We have studied the sensitivity of BETHY process parameters using a carbon-cycle data assimilation system to choices of atmospheric concentration network, high frequency terrestrial fluxes, and the choice of flux measurement network. Our conclusions can be summarized as follows:

- Observations of CO<sub>2</sub> concentrations allow us to strongly constrain the parameters relevant for net flux NEP but less for gross fluxes such as GPP. This problem is not greatly ameliorated by including high-frequency observations of flux since the relevant concentration signatures of high-frequency biosphere responses are spatially confined to the continents, whereas most CO<sub>2</sub> concentration monitoring sites are located away from the continents and are therefore missed by this signal.
- Flux measurements can help to better constrain most of the parameters relevant for gross primary productivity and net primary productivity.

Like Kaminski et al. (2012b), we suggest a combined use of both CO<sub>2</sub> concentrations and flux measurement networks to foster constraining most of the parameters related to terrestrial fluxes.

**Supplementary material related to this article is available online at <http://www.atmos-chem-phys.net/13/10555/2013/acp-13-10555-2013-supplement.pdf>.**

*Acknowledgements.* We acknowledge the financial support of the European Commission through the IMECC Integrated Infrastructure Initiative (I3) project under the 6th Framework Program (contract number 026188). P. Rayner is in receipt of an ARC Professorial Fellowship (DP1096309). We thank the anonymous reviewers of this manuscript for their constructive comments.

Edited by: C. McNeil



The publication of this article is financed by CNRS-INSU.

## References

- Aubinet, M., Grelle, A., Ibrom, A., Rannik, U., Moncrieff, J., T. Foken, T., Kowalski, A. S., Martin, P. H., Berbigier, P., Bernhofer, Ch., Clement, R., Elbers, J., Granier, A., Grünwald, T., Morgenstern, K., Pilegaard, K., Rebmann, C., Snijders, W., Valentini, R., and Vesala, T.: Estimates of the annual net carbon and water exchange of forest: the EUROFLUX methodology, *Adv. Ecol. Res.*, 30, 114–173, 2000.
- Baldocchi, D. D.: Assessing the eddy covariance technique for evaluating carbon dioxide exchange rates of ecosystems: past, present and future, *Glob. Change Biol.*, 9, 479–492, 2003.
- Baker, D. F., Law, R. M., Gurney, K. R., Rayner, P., Peylin, P., Denning, A. S., Bousquet, P., Bruhwiler, L., Chen, Y.-H., Ciais, P., Fung, I. Y., Heimann, M., John, J., Maki, T., Maksyutov, S., Masarie, K., Prather, M., Pak, B., Taguchi, S., and Zhu, Z.: TransCom 3 inversion intercomparison: Impact of transport model errors on the interannual variability of regional CO<sub>2</sub> fluxes, 1988–2003, *Global Biogeochem. Cy.*, 20, GB1002, doi:10.1029/2004GB002439, 2006.
- Carouge, C., Bousquet, P., Peylin, P., Rayner, P. J., and Ciais, P.: What can we learn from European continuous atmospheric CO<sub>2</sub> measurements to quantify regional fluxes – Part 1: Potential of the 2001 network, *Atmos. Chem. Phys.*, 10, 3107–3117, doi:10.5194/acp-10-3107-2010, 2010a.
- Carouge, C., Rayner, P. J., Peylin, P., Bousquet, P., Chevallier, F., and Ciais, P.: What can we learn from European continuous atmospheric CO<sub>2</sub> measurements to quantify regional fluxes – Part 2: Sensitivity of flux accuracy to inverse setup, *Atmos. Chem. Phys.*, 10, 3119–3129, doi:10.5194/acp-10-3119-2010, 2010b.
- Chevallier, F., Fisher, M., Peylin, P., Serrar, S., Bousquet, P., Bréon, F.-M., Chédin, A., and Ciais, P.: Inferring CO<sub>2</sub> sources and sinks from satellite observations: method and application to TOVS data, *J. Geophys. Res.*, 110, D24309, doi:10.1029/2005JD006390, 2005.
- Chevallier, F., Bréon, F.-M., and Rayner, P. J.: The contribution of the Orbiting Carbon Observatory to the estimation of CO<sub>2</sub> sources and sinks: Theoretical study in a variational data assimilation framework, *J. Geophys. Res.*, 112, D09307, doi:10.1029/2006JD007375, 2007.
- Chevallier, F., Ciais, P., Conway, T. J., Aalto, T., Anderson, B. E., Bousquet, P., Brunke, E. G., Ciattaglia, L., Esaki, Y., Fröhlich, M., Gomez, A. J., Gomez-Pelaez, A. J., Haszpra, L., Krummel, P., Langenfelds, R., Leuenberger, M., Machida, T., Maignan, F., Matsueda, H., Morguá, J. A., Mukai, H., Nakazawa, T., Peylin, P., Ramonet, M., Rivier, L., Sawa, Y., Schmidt, M., Steele, P., Vay, S. A., Vermeulen, A. T., Wofsy, S., and Worthy, D.: CO<sub>2</sub> surface fluxes at grid point scale estimated from a global 21-year reanalysis of atmospheric measurements, *J. Geophys. Res.*, 115, D21307, doi:10.1029/2010JD013887, 2010.
- Chevallier, F., Wang, T., Ciais, P., Maignan, F., Bocquet, M., Arain, A., Cescatti, A., Chen, J.-Q., Dolman, H., Law, B. E., Margolis, H. A., Montagni, L., and Moors, E. J.: What eddy-covariance flux measurements tell us about prior errors in CO<sub>2</sub>-flux inversion schemes, *Global Biogeochem. Cy.*, 26, GB1021, doi:10.1029/2010GB003974, 2012.
- Ciais, P., Reichstein, M., Viovy, N., Granier, A., Ogee, J., Allard, V., Aubinet, M., Buchmann, N., Bernhofer, C., Carrara, A., Chevallier, F., De Noblet, N., Friend, A. D., Friedlingstein, P., Grünwald, T., Heinesch, B., Keronen, P., Knohl, A., Krinner, G., Loustau, D., Manca, G., Matteucci, G., Miglietta, F., Ourcival, J. M., Papale, D., Pilegaard, K., Rambal, S., Seufert, G., Soussana, J. F., Sanz, M. J., Schulze, E. D., Vesala, T., and Valentini, R.: Europe-wide reduction in primary productivity caused by the heat and drought in 2003, *Nature*, 437, 529–533, 2005.
- Collatz G. J., Ribas-Carbo, M., and Berry, J. A.: Coupled photosynthesis-stomatal conductance model 5 of leaves for C4 plants, *Aust. J. Plant Physiol.*, 19, 519–538, 1992.
- Enting, I. G.: *Inverse Problems in Atmospheric Constituent Transport*, Cambridge University Press, 392 pp., 2002.
- Farquhar, G. D., Cammerer, S. V., and Berry, J. A.: A biochemical model of photosynthesis in leaves of C4 species, *Planta*, 149, 78–90, 1980.
- Foken, T. and Wichura, B.: Tools for quality assessment of surface-based flux measurements, *Agr. Forest Meteorol.*, 78, 83–105, 1996.
- Frankenberg, C., Fisher, J. B., Worden, J., Badgley, G., Saatchi, S. S., Lee, J.-E., Toon, G. C., Butz, A., Jung, M., Kuze, A., and Yokota, T.: New global observations of the terrestrial carbon cycle from GOSAT: Patterns of plant fluorescence with gross primary productivity, *Geophys. Res. Lett.*, 38, L17706, doi:10.1029/2011GL048738, 2011.
- Giering, R. and Kaminski, T.: Recipes for adjoint code construction, *ACM Transactions on Mathematical Software*, 24, 437–474, 1998.
- GLOBALVIEW-CO<sub>2</sub>: Cooperative Atmospheric Data Integration Project – Carbondioxide [CD-ROM], Global Monit. Div. Earth Syst. Res. Lab., NOAA, Boulder, Colorado (available at ftp://ftp.cmdl.noaa.gov/ccg/co2/GLOBALVIEW), 2004.
- Gurney, K. R., Law, R. M., Denning, A. S., Rayner, P. J., Baker, D., Bousquet, P., Bruhwiler, L., Chen, Y. H., Ciais, P., Fan, S. M., Fung, I. Y., Gloor, M., Heimann, M., Higuchi, K., John, J., Kowalczyk, E., Maki, T., Maksyutov, S., Peylin, P., Prather, M., Pak, B. C., Sarmiento, J., Taguchi, S., Takahashi, T., and Yuen,

- C. W.: Towards robust regional estimates of CO<sub>2</sub> sources and sinks using atmospheric transport models, *Nature*, 415, 626–630, 2002.
- Gurney, K. R., Law, R. M., Denning, A. S., Rayner, P. J., Baker, D., Bousquet, P., Bruhwiler, L., Chen, Y. H., Ciais, P., Fan, S. M., Fung, I. Y., Gloor, M., Heimann, M., Higuchi, K., John, J., Kowalczyk, E., Maki, T., Maksyutov, S., Peylin, P., Prather, M., Pak, B. C., Sarmiento, J., Taguchi, S., Takahashi, T., and Yuen, C. W.: TransCom 3 CO<sub>2</sub> inversion intercomparison: 30 1. Annual mean control results and sensitivity to transport and prior fluxes, *Tellus B*, 55, 555–579, doi:10.1034/j.1600-0889.2003.00049.x, 2003.
- Gurney, K. R., Law, R. M., Denning, A. S., Rayner, J. P., Pak, B. C., Baker, D., Bousquet, P., Bruhwiler, L., Chen, Y. H., Ciais, P., Fung, I. Y., Heimann, M., John, J., Maki, T., Maksyutov, S., Peylin, P., Prather, M., and Taguchi, S.: Transcom 3 inversion intercomparison: Model mean results for the estimation of seasonal carbon sources and sinks, *Global Biogeochem. Cy.*, 18, GB1010, doi:10.1029/2003GB002111, 2004.
- Hagen, S. C., Braswell, B. H., Linder, E., Frohling, S., Richardson, A. D., and Hollinger, D. Y.: Statistical uncertainty of eddy flux – based estimates of gross ecosystem carbon exchange at Howland Forest, Maine, *J. Geophys. Res.*, 111, D08S03, doi:10.1029/2005JD006154, 2006.
- Hardt, M. and Scherbaum, F.: The design of optimum networks for aftershock recordings, *Geophysical Journal International*, 117, 716–726, doi:10.1111/j.1365-246X.1994.tb02464.x, 1994.
- Heimann, M. and Körner, S.: The global atmospheric tracer model TM3, in: Max-Planck-Institut für Biogeochemie, Technical Report. Vol. 5, Max-Planck-Institut für Biogeochemie, Jena 131 pp. 131 [BGC0601; ECO140/036+5], 2003.
- Hourdin, F., Musat, I., Bony, S., Braconnot, P., Codron, F., Dufresne, J. L., Fairhead, L., Filiberti, M., Friedlingstein, P., Grandpeix, J., Krinner, G., LeVan, P., Zhao-Xin, L., and Lott, F.: The LMDZ4 general circulation model: climate performance and sensitivity to parametrized physics with emphasis on tropical convection, *Climate Dynam.*, 27, 787–813, 2006.
- Kaminski, T. and Rayner, P. J.: Assimilation and network design, in: *Observing the continental scale Greenhouse Gas Balance of Europe*, edited by: Dolman, H., Freibauer, A., and Valentini, R., Ecological Studies, chapter 3, 33–52, Springer-Verlag, New York, 2008.
- Kaminski, T., Heimann, M., and Giering, R.: A coarse grid three-dimensional global inverse model of the atmospheric transport, 2, Inversion of the transport of CO<sub>2</sub> in the 1980s, *J. Geophys. Res.*, 104, 18555–18581, 1999.
- Kaminski, T., Knorr, W., Rayner, P., and Heimann, M.: Assimilating atmospheric data into a terrestrial biosphere model: A case study of the seasonal cycle, *Global Biogeochem. Cy.*, 16, 1066, doi:10.1029/2001GB001463, 2002.
- Kaminski, T., Giering, R., Scholze, M., Rayner, P., and Knorr, W.: An example of an automatic differentiation-based modelling system, in: *Computational Science – ICCSA 2003*, edited by: Kumar, V., Gavrilova, L., Tan, C. J. K., and L'Ecuyer, P., International Conference Montreal, Canada, May 2003, Proceedings, Part II, volume 2668 of Lecture Notes in Computer Science, 95–104, Berlin, Springer, 2003.
- Kaminski, T., Scholze, M., and Houweling, S.: Quantifying the Benefit of A-SCOPE Data for Reducing Uncertainties in Terrestrial Carbon Fluxes in CCDAS, *Tellus B*, 62, 784–796, 2010.
- Kaminski, T., Knorr, W., Scholze, M., Gobron, N., Pinty, B., Giering, R., and Mathieu, P.-P.: Consistent assimilation of MERIS FAPAR and atmospheric CO<sub>2</sub> into a terrestrial vegetation model and interactive mission benefit analysis, *Biogeosciences*, 9, 3173–3184, doi:10.5194/bg-9-3173-2012, 2012a.
- Kaminski, T., Rayner, P. J., Voßbeck, M., Scholze, M., and Koffi, E.: Observing the continental-scale carbon balance: assessment of sampling complementarity and redundancy in a terrestrial assimilation system by means of quantitative network design, *Atmos. Chem. Phys.*, 12, 7867–7879, doi:10.5194/acp-12-7867-2012, 2012b.
- Kato, T., Knorr, W., Scholze, M., Veenendaal, E., Kaminski, T., Kattge, J., and Gobron, N.: Simultaneous assimilation of satellite and eddy covariance data for improving terrestrial water and carbon simulations at a semi-arid woodland site in Botswana, *Biogeosciences*, 10, 789–802, doi:10.5194/bg-10-789-2013, 2013.
- Knorr, W.: Annual and interannual CO<sub>2</sub> exchanges of the terrestrial biosphere: process-based simulations and uncertainties, *Global Ecology and Biogeography*, 9, 225–252, 2000.
- Knorr, W. and Kattge, J.: Inversion of terrestrial ecosystem model parameter values against eddy covariance measurements by Monte Carlo sampling, *Glob. Change Biol.*, 11, 1333–1351, 2005.
- Knorr, W., Kaminski, T., Scholze, M., Gobron, N., Pinty, B., Giering, R., and Mathieu, P.-P.: 20 Carbon cycle data assimilation with a generic phenology model, *J. Geophys. Res.*, 115, G04017, doi:10.1029/2009JG001119, 2010.
- Koffi, E. N., Rayner, P., Scholze, M., and Beer, C.: Atmospheric constraints on gross primary productivity and net ecosystem productivity: Results from a carbon-cycle data assimilation system, *Global Biogeochem. Cy.*, 26, GB1024, doi:10.1029/2010GB003900, 2012.
- Kuppel, S., Peylin, P., Chevallier, F., Bacour, C., Maignan, F., and Richardson, A. D.: Constraining a global ecosystem model with multi-site eddy-covariance data, *Biogeosciences*, 9, 3757–3776, doi:10.5194/bg-9-3757-2012, 2012.
- Lauvaux, T., Pannekoucke, O., Sarrat, C., Chevallier, F., Ciais, P., Noilhan, J., and Rayner, P. J.: Structure of the transport uncertainty in mesoscale inversions of CO<sub>2</sub> sources and sinks using ensemble model simulations, *Biogeosciences*, 6, 1089–1102, doi:10.5194/bg-6-1089-2009, 2009a.
- Lauvaux T., Gioli, B., Sarrat, C., Rayner, P. J., Ciais, P., Chevallier, F., Noilhan, J., Miglietta, F., Brunet, Y., Ceschia, E., Holman, H., Elbers, J. A., Gerbig, C., Hutjes, R., Jarosz, N., Legain, D., and Uliasz, M.: Bridging the gap between atmospheric concentrations and local ecosystem measurements, *Geophys. Res. Lett.*, 36, L19809, doi:10.1029/2009GL039574, 2009b.
- Law, R. M., Yu-Chan, C., Gurney, K. R., Rayner, P., Denning, A. S., and TransCom3 modelers: TransCom 3 CO<sub>2</sub> inversion intercomparison: 2. Sensitivity of annual mean results to data choices, *Tellus*, 55B, 580–595, doi:10.1034/j.1600-0889.2003.00053.x, 2003.
- Lasslop, G., Reichstein, M., Kattge, J., and Papale, D.: Influences of observation errors in eddy flux data on inverse model parameter estimation, *Biogeosciences*, 5, 1311–1324, doi:10.5194/bg-5-1311-2008, 2008.

- Lasslop, G., Reichstein, M., Papale, D., Richardson, A., Arneth, A., Barr, A., Stoy, P., and Wohlfahrt, G.: Separation of net ecosystem exchange into assimilation and respiration using a light response curve approach: critical issues and global evaluation, *Glob. Change Biol.*, 16, 187–208, 2010.
- Medvigy, D., Wofsy, S. C., Munger, J. W., Hollinger, D. Y., and Moorcroft, P. R.: Mechanistic scaling of ecosystem function and dynamics in space and time: Ecosystem Demography model version 2, *J. Geophys. Res.*, 114, G01002, doi:10.1029/2008JG000812, 2009.
- Moore, D. J. P., Hu, J., Sacks, W. J., Schimel, D. S., and Monson, R. K.: Estimating transpiration and the sensitivity of carbon uptake to water water availability in a subalpine forest using a simple ecosystem process model informed by measured net CO<sub>2</sub> and H<sub>2</sub>O fluxes, *Agr. Forest Meteorol.*, 148, 1467–1477, doi:10.1016/j.agrformet.2008.04.013, 2008.
- Nijssen, B., Schnur, R., and Lettenmaier, D.: Retrospective estimation of soil moisture using the VIC land surface model, 1980–1993, *J. Climate*, 14, 1790–1808, 2001.
- Papale, D., Reichstein, M., Aubinet, M., Canfora, E., Bernhofer, C., Kutsch, W., Longdoz, B., Rambal, S., Valentini, R., Vesala, T., and Yakir, D.: Towards a standardized processing of Net Ecosystem Exchange measured with eddy covariance technique: algorithms and uncertainty estimation, *Biogeosciences*, 3, 571–583, doi:10.5194/bg-3-571-2006, 2006.
- Peters, W., Jacobson, A. R., Sweeney, C., Andrews, A. E., Conway, T. J., Masarie, K., Miller, J. B., Bruhwiler, L. M. P., P'etron, G., Hirsch, A. I., Worthy, D. E. J., van der Werf, G. R., Randerson, J. T., Wennberg, P. O., Krol, M. C., and Tans, P. P.: An atmospheric perspective on North American carbon dioxide exchange: CarbonTracker, *P. Natl. Acad. Sci. USA*, 104, 18925–18930, 2007.
- Peters, W., Krol, M. C., Werf van der, G. R., Houweling, S., Jones, C. D., Hughes, J., Schaefer, K., Masarie, K. A., Jacobson, A. R., Miller, J. B., Cho, C. H., Ramonet, M., Schmidt, M., Ciattaglia, L., Apadula, F., Heltai, D., Meinhardt, F., Sarra, A. G., di Piacentino, S., Sferlazzo, D., Aalto, T., Hatakka, J., Ström, J., Haszpra, L., Meijer, H. A. J., Laan, S., van der Neupert, R. E. M., Jordan, A., Rodó, X., Morguá, J.-A., Vermeulen, A. T., Popa, E., Rozanski, K., Zimnoch, M., Manning, A. C., Leuenberger, M., Uglietti, C., Dolman, H., Ciais, P., Heimann, M., and Tans, P. P.: Seven years of recent European net terrestrial carbon dioxide exchange constrained by atmospheric observations, *Glob. Change Biol.*, 16, 1317–1337, doi:10.1111/j.1365-2486.2009.02078.x, 2010.
- Peylin, P., Bousquet, P., Le Quere, C., Sitch, S., Friedlingstein, P., McKinley, G., Gruber, N., Rayner, P., and Ciais, P.: Multiple constraints on regional CO<sub>2</sub> flux variations over land and oceans, *Global Biogeochem. Cy.*, 19, GB1011, doi:10.1029/2003GB002214, 2005.
- Piao, S. L., Ciais, P., Friedlingstein, P., Peylin, P., Reichstein, M., Luyssaert, S., Margolis, H., Fang, J. Y., Barr, A., Chen, A. P., Grelle, A., Hollinger, D. Y., Laurila, T., Lindroth, A., Richardson, A. D., and Vesala, T.: Net carbon dioxide losses of northern ecosystems in response to autumn warming, *Nature*, 451, 49–U43, 2008.
- Rayner, P. J.: The current state of carbon-cycle data assimilation, *Current Opinion in Environmental Sustainability*, 2, 289–296, doi:10.1016/j.cosust.2010.05.005, 2010.
- Rayner, P., Scholze, M., Knorr, W., Kaminski, T., Giering, R., and Widmann, H.: Two decades of terrestrial Carbon fluxes from a Carbon Cycle Data Assimilation System (CCDAS), *Global Biogeochem. Cy.*, 19, GB2026, doi:10.1029/2004GB002254, 2005.
- Rayner, P. J., Law, R. M., Allison, C. E., Francey, R. J., Trudinger, C. M., and Pickett-Heaps, C.: Interannual variability of the global carbon cycle (1992–2005) inferred by inversion of atmospheric CO<sub>2</sub> and  $\delta^{13}\text{C}_{\text{CO}_2}$  measurements, *Global Biogeochem. Cy.*, 22, GB3008, doi:10.1029/2007GB003068, 2008.
- Rebmann, C., Göckede, M., Foken, T., Aubinet, M., Aurela, M., Berbigier, P., Bernhofer, C., Buchmann, N., Carrara, A., Cescatti, A., Ceulemans, R., Clement, R., Granier, J. A., Grünwald, T., Guyon, D., Havránková, K., Heinesch, B., Knohl, A., Laurila, T., Longdoz, B., Marcolla, B., Markkanen, T., Miglietta, F., Moncrieff, J., Montagnani, L., Moors, E., Nardino, M., Ourcival, J.-M., Rambal, S., Rannik, U., Rotenberg, E., Sedlak, P., Unterhuber, G., Vesala, T., and Yakir, D.: Quality analysis applied on eddy covariance measurements at complex forest sites using footprint modelling, *Theor. Appl. Climatol.*, 80, 121–141, 2005.
- Reichstein, M., Falge, E., Baldocchi, D., Papale, D., Aubinet, M., Berbigier, P., Bernhofer, C., Buchmann, N., Gilmanov, T., Granier, A., Grunwald, T., Havrankova, K., Ilvesniemi, H., Janous, D., Knohl, A., Laurila, T., Lohila, A., Loustau, D., Mat-teucci, G., Meyers, T., Miglietta, F., Ourcival, J.-M., Pumpanen, J., Rambal, S., Rotenberg, E., Sanz, M., Tenhunen, J., Seufert, G., Vaccari, F., Vesala, T., Yakir, D., and Valentini, R.: On the separation of net ecosystem exchange into assimilation and ecosystem respiration: review and improved algorithm, *Glob. Change Biol.*, 11, 1424–1439, 2005.
- Richardson, A. D. and Hollinger, D. Y.: Statistical modeling of ecosystem respiration using eddy covariance data: Maximum likelihood parameter estimation, and Monte Carlo simulation of model and parameter uncertainty, applied to three simple models, *Agr. Forest Meteorol.*, 131, 191–208, 2005.
- Richardson, A. D., Mahecha, M. D., Falge, E., Kattge, J., Moffat, A. M., Papale, D., Reichstein, M., Stauch, V. J., Braswell, B. H., Churkina, G., Kruijt, B., and Hollinger, D. Y.: Statistical properties of random CO<sub>2</sub> flux measurement uncertainty inferred from model residuals, *Agr. Forest Meteorol.*, 148, 38–50, 2008.
- Richardson, A. D., Williams, M., Hollinger, D. Y., Moore, D. J. P., Bryan, P. D. B., Davidson, E. A., Scott, N. A., Evans, R. S., Hughes, H., Lee, J. T., Rodrigues, C., and Savage, K.: Estimating parameters of a forest ecosystem C model with measurements of stocks and fluxes as joint constraints, *Oecologia*, 164, 25–40, 2010.
- Rödenbeck, C., Houweling, S., Gloor, M., and Heimann, M.: CO<sub>2</sub> flux history 1982–2001 inferred from atmospheric data using a global inversion of atmospheric transport, *Atmos. Chem. Phys.*, 3, 1919–1964, doi:10.5194/acp-3-1919-2003, 2003.
- Scholze, M., Kaminski, T., Rayner, P., Knorr, W., and Giering, R.: Propagating uncertainty through prognostic CCDAS simulations, *J. Geophys. Res.*, 112, D17305, doi:10.1029/2007JD008642, 2007.
- Tarantola, A.: *Inverse Problem Theory: Methods for Data Fitting and Parameter Estimation*, Elsevier, Amsterdam, 1987.
- Tarantola, A.: *Inverse problem theory and methods for model parameters estimation*. Society for Industrial and Applied Mathematics, Philadelphia, ISBN 0-89871-572-5, 2005.

- Wang, Y. P., Leuning, R., Cleugh, H., and Coppin, P. A.: Parameter estimation in surface exchange models using non-linear inversion: How many parameters can we estimate and which measurements are most useful?, *Glob. Change Biol.*, 7, 495–510, 2001.
- Williams, M., Richardson, A. D., Reichstein, M., Stoy, P. C., Peylin, P., Verbeeck, H., Carvalhais, N., Jung, M., Hollinger, D. Y., Kattge, J., Leuning, R., Luo, Y., Tomelleri, E., Trudinger, C. M., and Wang, Y. -P.: Improving land surface models with FLUXNET data, *Biogeosciences*, 6, 1341–1359, doi:10.5194/bg-6-1341-2009, 2009.
- Ziehn, T., Kattge, J., Knorr, W., and Scholze, M.: Improving the predictability of global CO<sub>2</sub> assimilation rates under climate change, *Geophys. Res. Lett.*, 38, L10404, doi:10.1029/2011GL047182, 2011.
- Zobitz, J. M., Moore, D. J. P., Sacks, W. J., Monson, R. K., Bowling, D. R., and Schimel, D. S.: Integration of process-based soil respiration models with whole-ecosystem CO<sub>2</sub> measurements, *Ecosystems*, 11, 250–269, doi:10.1007/s10021-007-9120-1, 2008.
- Zupanski, D., Denning, A. S., Uliasz, M., Zupanski, M., Schuh, A. E., Rayner, P. J., Peters, W., and Corbin, K. D.: Carbon flux bias estimation employing Maximum Likelihood Ensemble Filter (MLEF), *J. Geophys. Res.*, 112, D17107, doi:10.1029/2006JD008371, 2007.